An Analytical quasi 2D steady-state Francis turbine model using first principles

To cite this article: P-T Storli and C Trivedi 2022 *IOP Conf. Ser.: Earth Environ. Sci.* **1079** 012006

An Analytical quasi 2D steady-state Francis turbine model using first principles

P-T Storli[1,2], **C Trivedi**[1]

[1] The Waterpower Laboratory, Alfred Getz' vei 4 N-7034 Dept. of Energy and Process Engineering, Norwegian University of Science and Technology.
[2] Corresponding author, pal-tore.storli@ntnu.no

Abstract: Accurate models are required for obtaining accurate simulation results. High fidelity numerical models exist, but for the simulations of large hydropower conduit systems one-dimensional (1D) models are still required. For the operation and characteristics of hydraulic machinery the state variables in 1D pipe computation are not necessarily providing sufficient level of detail on what happens inside the machine to accurately predict component and system behaviour. This work is looking into the physics of the spatial distribution of the flow at the outlet of a Francis turbine runner in order to include 2D effects into a 1D analysis. The key finding is a differential equation describing the distribution of the relative velocity W between the flow and the runner outlet, which enables numerical integrating for finding the distribution of W itself, and subsequently the circumferential and meridional components needed to execute the integrals turning the 2D results into functions of the 1D state variables. The presented work is reflecting condition at the best efficiency point, but ongoing work is expanding this to map the entire region of a turbine runner. The approach should be very relevant for future implementations into digitalization schemes such as digital twins

1. Introduction

Simulations are an important tool for investigation of transients and dynamic behaviour of systems. For hydraulic systems, the characteristics of hydraulic machinery are important for the simulation results and their reliability. If experimental results are not available for the characteristics, a model must be used. Actually, a model is preferred over experimental results because such results are obtained from steady-state measurements, where all dynamic effects are excluded. The drawback of a model is that losses are possibly not properly implemented.

Even in 2022 the costs of computational power and time are so high that a highly resolved CFD simulation of a turbine unit for the purpose of dynamic simulations of hydropower operation is too high, let alone including 3D or even 2D models of the entire hydraulic system being simulated. This is a problem for the further development of applications such as digital twins and further digitalization. The problem can be addressed in two ways; speeding up the highly resolved CFD simulations or improving the quality of the simpler representations of complex components in the system. This work is oriented towards the latter.

The work presented is seeking to find a model of a hydraulic turbine for the use in simulations of hydropower operation. The model is based on first principles and rely on the velocity distribution at the outlet region of the turbine runner, more specifically where the flow has been completely diverted into axial flow in the draft tube cone section. To be able to find this velocity distribution a differential equation describing the relative velocity between fluid and runner at such outlet section is established. This equation is not analytically solvable (to the current knowledge of the authors, that is), and is numerically solved by performing a Euler integration. A 'goal seek' procedure is then performed where the starting value for the relative velocity is changed, and the desired flow is the target for the procedure. The relative velocity is then used to find the meridional (for the analysed cross section assumed to be the axial velocity) and the circumferential velocity components of the absolute velocities, as these ones are required in the analysis. To verify that the velocity distributions are ballpark, inviscid numerical simulations have been performed on the Francis99 model runner at NTNU. The results agree well, and the distributions of the velocity components are combined to form the expression for local angular momentum, which then is integrated across the outlet section giving rise to the "quasi 2D" terminology in this paper's title.

Having the velocity distribution at the outlet available presents many interesting possibilities. First, it can be used to find the pressure distribution at the outlet. Knowing the velocity- and pressure distributions the efficiency can be found, as the head over the machine can be determined. This is subject to losses being included in the analysis. The "turbine" is according to standards defined between the spiral casing inlet and the draft tube outlet, and since the investigated runner outlet cross section is the boundary to the draft tube cone and subsequently also the draft tube elbow more detailed information of the conditions in these components can open for implementation of more detailed description of losses, and even the possibility of identifying and including the effects of things like part load vortex rope and high load vortex cavity in a 1D simulation.

Many different models exist, and many of them are using the Euler turbine and pump equation, which is often referred to as a 1D equation since it is only required to have information on the variables included in a so-called 1D simulation of fluid flow (combined with geometrical values of the runner, that is), meaning the flow Q through the unit and the head H removed from the flow through the unit [1-6]. This 1D version is obtained if the assumption of constant angular momentum at the turbine outlet section is applied to the more physically correct integration of the flux of angular momentum at the outlet. This assumption is avoided in this work and leads to the new model containing more detailed information, despite the intention of ultimately being used in a 1D representation of the dynamics.

A model for the use in a 1D simulation of hydraulic and mechanical rotating domains must link the head, flow, torque, and rotational speed to each other. Finding this using first principles we must turn to the fundamental governing equations for the motion of fluids.

2. Governing equations and the relative velocity *W*

The governing equations for all incompressible flows are the equations of motion; The Navier-Stokes equation and equation of continuity (The latter will not be elaborated in this paper). For inviscid flows, the Navier-Stokes equation loses the term describing viscous effects and becomes the Euler equation[7]

$$\frac{D\vec{V}}{Dt} = \vec{a}_{abs} = \frac{\partial \vec{V}}{\partial t} + \left(\vec{V}\nabla\right)\vec{V} = -\frac{\nabla p}{\rho} + \vec{\mathrm{X}} \qquad (1)$$

Where $\vec{V}$ is the absolute velocity vector, t is the time, ∇p is the pressure gradient and ρ is the constant fluid density. The last term $\vec{X}$ is representing the body forces acting on the fluid parcel that is accelerating and often the only body force considered is the gravity, leading to $\vec{X} = \vec{g}$. However, in the case of a conservative system, the body force may also be considered to be the gradient of a potential function, ie $\vec{X} = -\nabla\varphi$ [7]. Expanding these equations using a cylindrical coordinate system ($\vec{V} = V_r\overrightarrow{e_r} + V_\theta\overrightarrow{e_\theta} + V_z\overrightarrow{e_z}$) we get one equation for each of the directions, but we will focus on the equation that investigate the radial acceleration, and rearranging we get an expression for the pressure gradient in the radial direction:

$$\frac{1}{\rho}\frac{\partial p}{\partial r} = -a_{abs,r} - \frac{\partial \varphi}{\partial r} = -\left(\frac{\partial V_r}{\partial t} + V_r\frac{\partial V_r}{\partial r} + \frac{V_\theta}{r}\frac{\partial V_r}{\partial \theta} - \frac{V_\theta^2}{r} + V_z\frac{\partial V_r}{\partial z}\right) - \frac{\partial \varphi}{\partial r} \qquad (2)$$

The potential function turns out to be the angular momentum itself (the classical assumption used when analysing turbomachinery when the blades have been assumed to be infinitely thin and infinitely many), $\varphi = uV_\theta = \omega r V_\theta$ [8]. The pressure gradient can be integrated to get the pressure difference in the radial direction. Another expression for the pressure difference between two points along a (relative) streamline can be obtained using the Rothalpy equation, i.e. the Bernoulli equation in a rotating frame of reference [9]. This can be done for the outlet of the runner, as seen in figure 4. Combining these expressions along with assumptions used for the outlet of the runner we can derive an expression for the relative velocity W at the outlet.

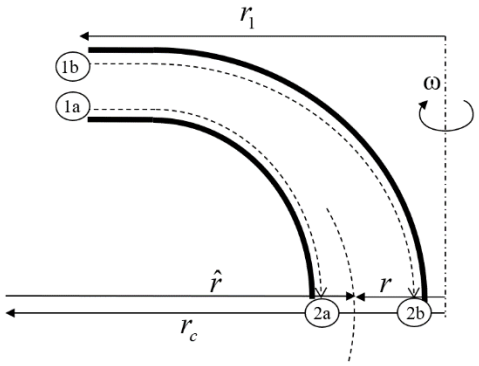

Figure 1: Schematics of the figure used to obtain the expression for V_m and V_θ

This work can be seen in Appendix A, and the resulting expression for W is a differential equation:

$$\frac{dW}{dr} = \frac{W^2\left(\frac{sin^2\beta}{r_c - r} - \frac{cos^2\beta}{r}\right) - \omega W cos\beta + 2\omega^2 r}{(W - \omega r cos\beta)} \tag{3}$$

Finding W from this differential equation is not a trivial task. However, a distribution for W can be found using a numerical Euler integration, if the distribution of the angle β is known. Since we are investigating a cross section which is different from where the actual outlet of the blades is, we cannot say that the distribution of the angles at the cross-section under investigation is equal to the distribution at the outlet of the blades. For the work presented here the flow angles found from the results of the CFD analysis is used as the β distribution in the above equation. The numerical simulations are described in Appendix B. When having W and the flow angle, other velocity components needed can be found using the trigonometric equations, which we shall see is important to establish the model. The model is established by describing the temporal acceleration of the flow Q through the turbine as a function of the sum of head (linear momentum consideration) and the acceleration of the rotational speed as a function of the sum of the torques (angular momentum consideration). We will start with the latter.

3. Torque: The angular momentum equation

The angular momentum equation is the equivalent of the linear momentum equation for angular motion. In words, it describes that the sum of the time rate of the change of angular momentum of the water inside a control volume and the net flux of angular momentum out of a control volume must be equal to the sum of all the external torques acting on the control volume, as seen in Eq. 4 [9]:

$$\sum \vec{M}_{external} = \underbrace{\frac{d}{dt}\int_{CV} \rho(\vec{r} \times \vec{V}) d\forall}_{\text{time rate of change of AM in CV}} + \underbrace{\int_{CS} \rho(\vec{r} \times \vec{V})(\vec{V_r} \cdot \vec{n}) dA}_{\text{Net flux of AM out of CV}} \tag{4}$$

Our CV is placed outside the outer geometry of a Francis turbine runner, as seen in Figure 2 and Figure 3. Considering steady state conditions and a CV of fixed size, only the net flux integral remains.

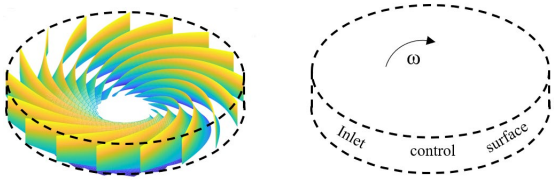

Figure 2: Control Volume CV (inside the control surface, CS) and the runner blade cascade of a Francis runner viewing the inlet CS

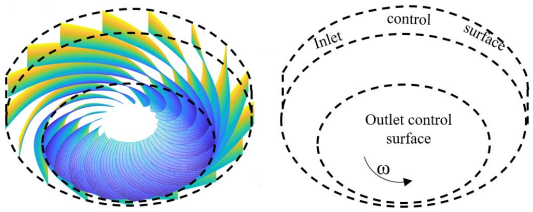

Figure 3: Control Volume CV (inside the control surface, CS) and the runner blade cascade of a Francis runner viewing both inlet and outlet CS

In this work we will use a coordinate system where the positive z-axis is defined pointing upwards, so the normal vector of the outlet cross section area is pointing in the negative z direction. Following this, the ω as drawn in Fig. 2 and 3 has a negative value.

3.1. Net flux of AM out of CV

The net flux integral is a vector integral, and the vector integrated is the cross product of the radii vector and the velocity vector. This is evaluated easiest in a cylindrical coordinate system described by unit vectors $\overrightarrow{e_r}$, $\overrightarrow{e_\theta}$ and $\overrightarrow{e_z}$. The cross product becomes

$$\vec{r} \times \vec{V} = -rV_z\overrightarrow{e_\theta} + rV_\theta\overrightarrow{e_z} \tag{5}$$

The only term contributing to rotational motion is the z-component, so this is the only one we will continue to investigate

$$\int_{CS} \rho(\vec{r} \times \vec{V})_z(\overrightarrow{V_r} \cdot \vec{n})dA = \int_{CS} \rho r V_\theta (\overrightarrow{V_r} \cdot \vec{n})dA \tag{6}$$

Furthermore, the dot product between the relative velocity and the normal vector of the control surface is giving the magnitude of the velocity component carrying the mass over the surface. This is commonly called the meridional component in hydraulic machines. The dot product is therefore giving the magnitude of this velocity and including a sign depending on whether the relative velocity vector has a component in the same, or opposing, direction of the normal vector; $(\overrightarrow{V_r} \cdot \vec{n}) = -V_m$ for an inlet, and $(\overrightarrow{V_r} \cdot \vec{n}) = V_m$ for an outlet. Eq. 6 can then be divided into two integrals: One for the inlet (later using subscripts 1) and one for the outlet (later using subscripts 2),

$$\int_{CS} \rho r V_\theta (\overrightarrow{V_r} \cdot \vec{n})dA = -\int_{inlet} \rho r V_\theta V_m dA + \int_{oulet} \rho r V_\theta V_m dA \tag{7}$$

If the angular momentum is equal across the inlet and outlet, *this equation returns the torque which multiplied by angular velocity gives the left-hand side of the Euler pump and turbine equation expressed in unit power*. This assumption is not imposed on the work presented here, and the integrals must be further investigated. The integrals are best treated individually, and we'll start with the inlet integral.

3.2. Inlet flux integral

For the inlet CS, which is a cylindrical shell at constant radii, the rotor stator interaction and the potential flow effect of the guide vanes will give a periodicity of the magnitude of the V_θ component [10]. However, let us for simplicity assume that the V_θ is constant everywhere. The parenthesis term is carrying the information on the magnitude of the velocity that is normal to the CS surface, ie the velocity component commonly called the meridional velocity component. Noting the consequence of the direction of the normal vector on the sign discussed above, be aware that the property being carried by the flow might also have a negative sign, thus alter the sign once more. This is the case here, where the V_θ component is negative, as it is geometrically defined as $V_{\theta 1} = -V_1 cos\alpha_1 = -\frac{V_m}{tan\alpha_1} = -\frac{Q}{A_1 tan\alpha_1}$. If we assume a uniform distribution of the meridional velocity component at the inlet, the entire integrand

is a constant and we are only left with integrating dA, which simply returns the inlet area A_1. The density, meridional velocity and the area are multiplied to obtain the flow. Using all these assumptions, the inlet integral becomes

$$\int_1 \rho r_1 V_{\theta 1}(-V_m) dA = -\rho r_1 V_{\theta 1} Q_1 = \rho r_1 \frac{Q^2}{A_1 tan\alpha_1} \tag{8}$$

3.3. Outlet flux integral

The outlet of the control volume is a circular disk, and the radii is obviously not a constant at the outlet. Furthermore, the velocity component V_θ is generally not a constant across the cross section. This makes it impossible to assess the integral simply because the non-constant velocity components are not known a priori. When designing a turbine, the V_θ velocity component is often set to be zero, because this is the objective of the design; to have no swirl at the outlet thus extracting as much angular momentum from the flow as possible. This design criteria is typically using some assumption on the local V_m component of the flow and the known circumferential speed of the runner in order to choose blade angles which gives zero rotation at all outlet radii. At other operational points than the design point, the zero-rotation condition is surely not met, and we also need to have a description of this component. If we consider the assumption that the flow must leave the outlet of the runner blades in the direction of the blades, we can make a geometrical relation between the local blade angle β, local circumferential velocity of the blade outlet u, and the local velocity components of the absolute velocity; V_θ and V_m. This is seen in Figure 4. The link between them is, however, the relative velocity between the flow and the runner, W.

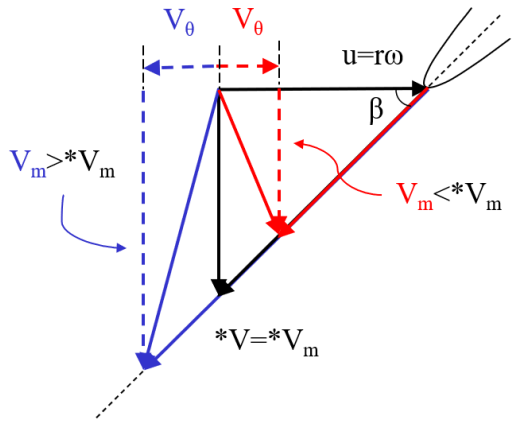

*Figure 4: Outlet velocity triangles at Q>*Q (corresponding to blue), Q=*Q (corr. To black) and Q<*Q (corr. To red)*

The other components can be determined using the knowledge of the radii, angular velocity and the blade angle, the latter being fixed after construction of a Francis runner. Mathematically, the relation for V_θ and V_m are described by

$$V_\theta = W\cos\beta + \omega r \tag{9}$$

$$V_m = W\sin\beta \tag{10}$$

Finding the relative velocity W is key to unlocking the velocity component necessary for completing the outlet integral from the AME equation, and as we have seen this has been found using the differential Eq. 3, which used information regarding the angle β. So, both W and β are known making the velocity components known as well. This makes it possible to evaluate the outlet flux integral expressed as

$$\int_{oulet} \rho r V_\theta V_m dA = \int_{outlet} \rho r(W\cos\beta + \omega r) W\sin\beta\, dA \tag{11}$$

Then we can complete the flux integrals by combining the inlet and outlet expressions:

$$\int_{CS} \rho(\vec{r} \times \vec{V})_z (\vec{V_r} \cdot \vec{n}) dA = \rho r_1 \frac{Q^2}{A_1 tan\alpha_1} + \int_{outlet} \rho r(W \cos\beta + \omega r) W \sin\beta \, dA \quad (12)$$

3.4. The final torque equation

Combining all terms from the original AME we end up with

$$\sum M_{z,external} = \rho r_1 \frac{Q^2}{A_1 tan\alpha_1} + \int_{outlet} \rho r(W \cos\beta + \omega r) W \sin\beta \, dA \quad (13)$$

We have not yet even discussed the left-hand side of the equation, which is dealing with so-called "external" torques. These torques are acting on the rotating control volume arising from other interactions than what is due to the flow in and out of the control volume. The biggest ones of these torques should be the torque acting on the rotating part by the generator, $M_{generator}$. The other ones are due to some kind of loss present in on the boundary of the control volume. These losses are typically disc friction losses due to shear forces in the water between stationary and rotating parts, and losses in bearings, both radial and axial, whatever present at the unit. The power dissipated by such losses are typically a function of the angular velocity cubed [11], thus the reduction in torque due to such losses will be a function of the angular velocity squared. All these external torques are positive as they are all trying to slow down the runner, i.e., reducing the negative value, thus accelerating it: a positive torque. The torque we are interested in describing is the generator torque, as this is the one which in turn is providing the power transformed into electricity. This leads to the AME equation giving us the below expression for the steady state generator torque:

$$M_{generator} = \rho r_1 \frac{Q^2}{A_1 tan\alpha_1} + \int_{outlet} \rho r(W \cos\beta + \omega r) W \sin\beta \, dA - (C_1 + C_2)\omega^2 \quad (14)$$

Where C_1 and C_2 are constants used to include the disc friction losses and bearing losses, respectively.

4. Head

"The head" of a turbine unit is defined as the difference in mechanical energy in unit meters (specific energy divided by the gravitational acceleration) from the inlet pipe to the outlet of the draft tube. We can also find this by knowledge of the individual physical phenomena that make up the total difference. Considered in this work is the head extracted by an ideal machine (the "perfect" turbine runner), and the losses due to friction in the runner, the losses due to inlet mismatch of flow and geometry often called incidence losses, and finally what is lost in the draft tube. This is seen in the equation below, and we will discuss these terms individually.

$$\rho g Q H = \rho g Q \left(H_{ideal\,machine} + h_{loss,friction} + h_{loss,incidence} + h_{loss,draft\,tube}\right) \quad (15)$$

4.1. The head of an ideal machine

The classical representation of lifting height of a pump, where subscript 1 indicates high-pressure side and subscript 2 indicates low-pressure side [11] is given in Eq. 16:

$$gH = \frac{C_1^2 - C_2^2}{2} + \frac{U_1^2 - U_2^2}{2} + \frac{W_2^2 - W_1^2}{2} \quad (16)$$

An ideal pump will work as an ideal turbine if the flow and rotation is reversed, so the equation is valid for an ideal turbine as well. The basis for this equation is the Euler pump and turbine equation, where the law of cosines has been applied to the velocity component to obtain the above relation. This is an important point because the implication to this is that no losses are included in this equation. Furthermore, there is a reason for concern when assessing the applicability of this equation for the work presented here. The simplification of the outlet integral leading to the Euler pump and turbine equation was not acceptable for the development of the torque equation, and it shouldn't be acceptable for the work on describing the head either. However, we will use the method that's used to obtain the Euler

pump and turbine equation, which is to say that the mechanical power transferred to the rotating domain is the same as the hydraulic power removed from the flow, implying a hydraulic efficiency equal to unity and a so-called "ideal machine". This means that

$$\rho g Q H_{ideal\ machine} = -\vec{M}_{generator} \cdot \vec{\omega} = -M_{generator}\vec{e_z} \cdot \omega\vec{e_z} = -M_{generator}\omega \tag{17}$$

Where the negative sign comes from the fact that when using the mechanical torque in this way we are including that this torque is balancing the driving torque from the flow, and is opposite in direction to this. Rearranging for $gH_{ideal\ machine}$ and substituting for $M_{generator}$ the terms that was obtained from the AME equation (disregarding the losses, aligning to the "ideal machine" assumption), we get

$$gH_{ideal\ machine} = -\omega r_1 \frac{Q}{A_1 tan\alpha_1} - \frac{1}{Q}\int_{outlet} \omega r(W\ cos\,\beta + \omega r)\, W\ sin\,\beta\ dA \tag{18}$$

4.2. Friction loss

The friction loss will always be present when a flow is going through a runner, and friction is dependent on relative velocity. A factor is multiplied with the relative velocity, and since for the presented work the factor will need to be calibrated, we can choose at which position to link it to. It is then convenient to link it to the inlet relative velocity W_1, and we get

$$gh_{friction} = \lambda W_1^2 \tag{19}$$

Where λ is a dimensionless head-loss coefficient. However, we will not look into detail on this because we are only investigating one operational point, and this point will have to be the one we use for calibration as well, so we will not get any verification or validation of this term still.

4.3. Incidence losses

There are also losses when there's a mismatch between the actual flow angle and the angle the runner is designed for, so-called incidence losses. These losses are complicated to represent accurately, because there's several effects arising due to a mismatch between these angles. It is likely that these losses are originating due to phenomena comparable to what is seen on a hydrofoil experiencing different angle of attacks, combined with cascade effects due to proximity of other foils. Still, such effects are not accurately quantified for the purpose of this work, but a loss proportional to the stagnation pressure of the relative velocity component normal to the physical blade inlet angle is assumed, as in [2].

$$gh_{incipient} = C_3 \frac{W_1^2 sin^2(\beta_1 - \beta_{1,design})}{2} \tag{20}$$

Where C_3 is a dimensionless head-loss coefficient. This makes the loss small for small values of the argument but increasing more rapidly when the angle increases more. The coefficient C_3 must be determined or calibrated, but for the work presented herein we conclude that the entire term describing the incidence losses is zero, since we are investigating the BEP where the flow angle and the design flow angle should be identical.

The last term of assumed importance when describing the losses for the turbine unit are the draft tube losses. Until now we have only considered effects in, and related to, the runner. But we must include losses in the draft tube as well as this, by definition, is a part of the hydraulic turbine.

4.4. Draft tube losses

The losses in the draft tube are also difficult to assess, and swirl in the flow is giving rise to several well-known physical phenomena, the rotating vortex rope and the vortex cavity being the most visual ones in lab setups. Friction is also present, and the detail of the flow is very much dependent on operating conditions. Typically, the efficiency of a draft tube is linked to a variable called the swirl number, and this variable is also used to indicate the existence of vortex phenomena. Not investigated any further in this work, it will be indicated as a symbol in the below equation. The development of the

mathematical representation of the draft tube losses below can be seen in Appendix C, assuming steady state conditions.

$$h_{loss,draft\ tube} = h_{loss,draft\ tube,z} + \frac{1}{\rho g Q}\int\limits_{\substack{inlet\\draft\ tube}}\left(\int\frac{\partial p}{\partial r}dr - \int\limits_{r=0}^{r_m}\frac{\partial p}{\partial r}dr + \rho\frac{V_m^2}{2}\right)V_m dA - \frac{Q^2}{2gA^2}_{\substack{inlet\\draft\ tube}} + h_{loss,swirl\ phenomena} \quad (21)$$

4.5. The head of the turbine unit

Combining all elements discussed in the head section, we end up with the head of the turbine unit for steady state conditions described as

$$\begin{aligned} gH_{turbine\ unit} &= gH_{ideal\ machine} + gh_{friction} + gh_{incipient} + gh_{loss,draft\ tube} \\ &= -\omega r_1\frac{Q}{A_1 tan\alpha_1} - \frac{1}{Q}\int_{outlet}\omega r(W\cos\beta + \omega r)\,W\sin\beta\,dA \\ &+ \lambda W_1^2 + C_3\frac{W_1^2 sin^2(\beta_1 - \beta_{1,design})}{2} + gh_{loss,draft\ tube,z} \\ &+ \frac{1}{\rho Q}\int\limits_{\substack{inlet\\draft\ tube}}\left(\int\frac{\partial p}{\partial r}dr - \int\limits_{r=0}^{r_m}\frac{\partial p}{\partial r}dr + \rho\frac{V_m^2}{2}\right)V_m dA \\ &- \frac{Q^2}{2A^2}_{\substack{inlet\\draft\ tube}} + gh_{loss,swirl\ phenomena} \end{aligned} \quad (22)$$

5. Results and discussion

The final goal of this work is to have a model which exhibits all familiar characteristics when used in transient simulations of a turbine and a hydraulic system. This is for the time being not how far the work has progressed. Currently we have compared with CFD results for one steady state operating point, namely the BEP of the Francis99 runner at NTNU. This is explained in Appendix B. The relative velocity distribution has been found using the condition that the flow (post-processes from using the relative flow distribution) is the same as for the CFD results. In practise, the starting value for the relative velocity distribution is changed so that the flow is the same as in the CFD results. The flow angle β between the relative velocity W and the circumferential component obtained from the CFD results are used in the equation for the relative velocity gradient and is seen in Figure 5.

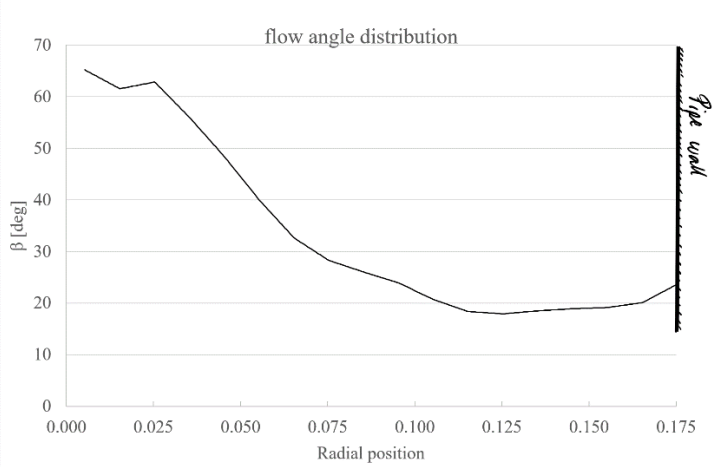

Figure 5: Distribution of the flow angle inside the pipe section

The spatial resolution of the scheme used to numerically integrate (Euler's method) the differential equation for W was using 340 equally spaced increments in radial position between 0,0053 m and 0,1753 m, making the increment in radial distance only 0,0005 m. Knowing the angle beta from the CFD results, the distribution of W could then be found assuming a starting value at r=0,0053m. The values for β were spaced farther apart in the numerical results so in between data points linear interpolation was used. When this was implemented the V_m component was found (Same as the Wm component), and the flow could then be found integrating the V_m component over the cross section. The value for the flow was then compared to the value for the CFD results, and if there was a mismatch the starting value for W was changed. This was performed using the "goal seek" function in Microsoft Excel. This function stopped when the integrated flow was Q= 0,26302 m3/s, while the target flow was Q=0,2629 m3/s. The CFD results were extracted some distance down into the draft tube cone, 0,243 m below the centre line of the inlet of the turbine. The reason for this is that one of the assumptions used to develop the differential equation for W was that there is no radial velocity component. We had to look a distance down into the draft tube cone to find where the radial component was as close to zero as possible for the purpose of comparing to the analytical results. For this reason, the f̂-value was chosen so big that it would mathematically mimic axial flow, so it was set to 500000, effectively cancelling all terms involving it from the differential equation.

5.1. Relative velocity W

The relative velocity *W* can be seen in Figure 6 on next page, along with the circumferential and meridional velocity components and pressures. The results from the analytical equations are shown as dash-dot lines, whereas the CFD results are shown in solid lines. For the CFD results the radial velocity component is shown, but no line for the analytical results is drawn as it has been assumed that the radial component is zero when the equations were developed.

Given the fact that the numerical results include real turbine geometry, and the analytical results only includes the angle from the numerical results, the match between the analytical and numerical results seems good. The largest deviation in the meridional component is close to the centre, and that's where the presence of the runner cone is influencing the flow, making the mismatch between the actual geometry and the assumption in the analytical equations greatest. At larger radii the meridional components match very well. The match between the circumferential components is not as good, in fact there are multiple regions where the rotation is in the opposite direction of each other. They are identical at the same radii as where the meridional components are identical, and when the analytical meridional component is smaller than the CFD result, the analytical circumferential velocity is higher than the CFD results, and vice versa. This is a cause for concern but remembering that this is at BEP and the flow rotation generally is small at this operational point, it is likely that the sign and magnitude of the circumferential component will be sensitive and differences will easily occur. The swirl number of the two flows are found to be S=-0,0387 for the CFD results, and S=0,0417 for the analytical counterpart. They're both small, but the most important difference is the sign.

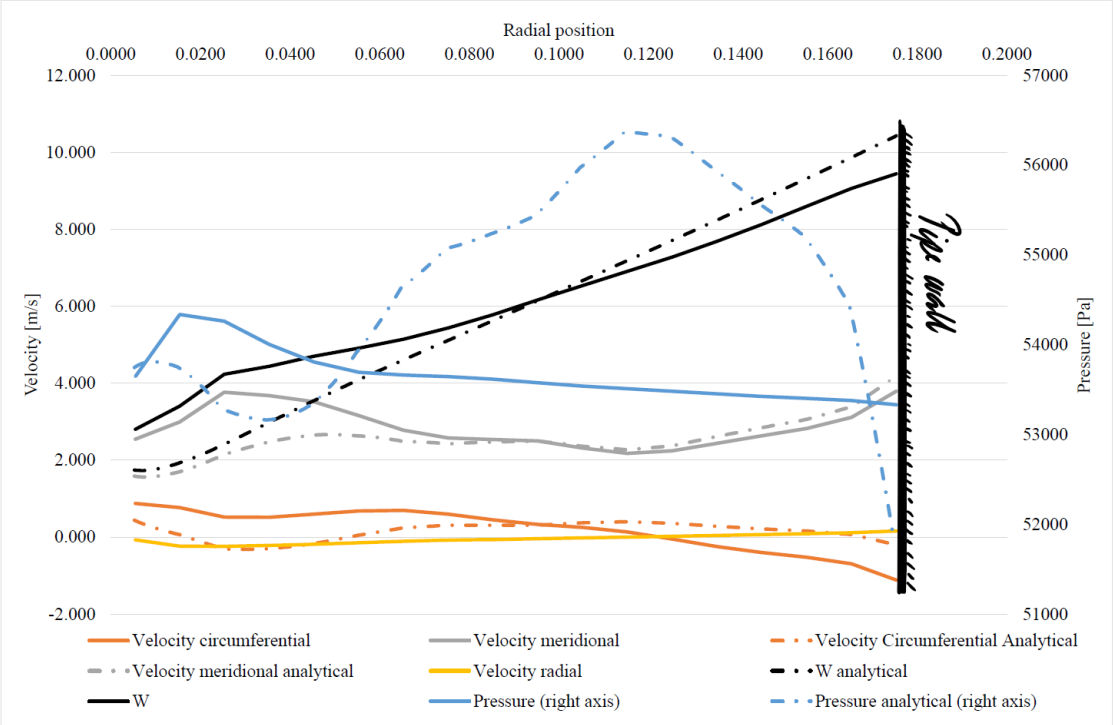

Figure 6: Velocities and pressure. For the CFD results W has been post-calculated using the formula $W = \sqrt{(V_\theta - \omega r)^2 + V_m^2}$, thus omitting the radial component. Solid lines are all numerical results.

5.2. Torque, head and efficiency

The torque is found using Eq. 14, but as the coefficients of the disc friction losses and bearing losses are not known they must be calibrated if the torque is to be compared to experimental results. The same issue is linked to the losses in the head of the unit, as they rely on coefficients not known a priori. Setting all the losses to zero, we can calculate the efficiency, and reassuringly it is computed and found to be unity:

$$\eta = \frac{-M\omega}{\rho g H_{ideal\ machine} Q} = \frac{-\omega r_1 \rho \frac{Q^2}{A_1 tan\alpha_1} - \rho \int_{outlet} \omega r (W\cos\beta + \omega r)\, W \sin\beta\, dA}{-\omega r_1 \rho \frac{Q^2}{A_1 tan\alpha_1} - \rho \int_{outlet} \omega r (W\cos\beta + \omega r)\, W \sin\beta\, dA} \equiv 1 \quad (23)$$

Not surprisingly this must be the case, and it only shows that unless some losses are mathematically included into the models of torque and head, you will always find an efficiency equal to 1 when performing desk top studies. If the torque and head are measured in experimental test the measurements include losses, and the efficiency will be less than 1. Guesstimates of the losses (linking to the chosen values for λ, C_1 and C_2) are included in a calculation example, see section 5.2.2 below.

5.2.1 Draft tube losses

The losses computed due to the pressure distribution at the inlet of the draft tube that comes in excess to the losses assuming axial flow can be computed, as everything required is known. Interestingly, it turns out to be negative;

$$\frac{1}{\rho Q} \int_{\substack{inlet \\ draft\ tube}} \left(\int \frac{\partial p}{\partial r} dr - \int_{r=0}^{r_m} \frac{\partial p}{\partial r} dr + \rho \frac{V_m^2}{2} \right) V_m dA = -0{,}42566\ [gh] \quad (24)$$

As this is only a part of the total loss for the draft tube, it is not automatically in violation of the first law of thermodynamics. The total loss for the draft tube must be positive for the first law of thermodynamics to be fulfilled, but the negative contribution is highly interesting as it is well known that it is beneficial to have a small rotation in a draft tube flow because this reduces the overall loss [12].

5.2.2 Calculation example

As an example of a full calculation as well as for the possibility of reviewing the equations, we give a calculation example. For the efficiency to be calculated one must have the values of λ, C_1 and C_2. These have been chosen arbitrarily within reasonable ranges for such coefficients. We also need to know the value for the friction in the draft tube, $gh_{loss,draft\ tube,z}$ and this has been assumed to be the same as the friction in the runner. These, together with required parameters, are given in Table 1. The value of W_1 used for this case is W_1=3,05 m/s, corresponding to the BEP value.

Using these numbers, together with the velocity components and flow angle distribution seen in Figure 5 obtained from the analytical approach, we get the efficiency:

$$\eta = \frac{-M\omega}{\rho g H_{turbine\ unit} Q} = \frac{74055{,}93}{79107{,}85} = 0{,}9361 \qquad (25)$$

Table 1: *Coefficients, parameters and constants (first row), their units (below) and their values (second row)*

λ	C_1	C_2	$gh_{loss,draft\ tube,z}$	r_1	A_1	α_1	r_2 (at z = -0,243	ω	ρ	r_m	Q	g
[-]	[Nms^2]	[Nms^2]	[m^2/s^2]	[m]	[m^2]	[°]	[m]	[rad/s]	[m^3/kg]	[m]	[m^3/s]	[m/s^2]
0,02	0,01	0,02	$= gh_{friction} = \lambda W_1^2$	0,315	0,087	10	0,1753	-55,68	998,5	0,14	0,2629	9,821

6. Conclusions

This paper presents ongoing work aiming to develop a dynamic model for a Francis turbine which has the possibility to include more detailed information than simple 1D models but omitting full CFD simulations and everything this entails. The key finding is an equation which describes the distribution of the relative velocity at the outlet of a Francis runner. Knowing this, the information required to perform 2D analysis by executing integrals appearing in the Angular Momentum Equation and Linear Momentum Equation becomes available. Executing these integrals will then give the added level of detail into the models of the turbine unit in a quasi 2D way for the 1D analysis. Furthermore, parameters used to classify the presence of different phenomena can be calculated, and models of those phenomena can be incorporated into the turbine model. The work seems to be very relevant for the topic of digital twins for hydropower plants.

7. Further Work

Much work is needed before the model can be considered complete. Until now, only the Best Efficiency operation Point has been investigated, as well as steady state conditions. The real test of any model is at off-design operating conditions, so this will be investigated, as well as including the unsteady terms in the model. Furthermore, it is paramount that it is possible to include the a priori known distribution of the outlet angle a runner rather than what is done in this work; using the flow angle from a CFD simulation. Including swirl phenomena linked to the swirl number is also something that will extend the model's applicability.

Acknowledgements

This work has partly been funded by FME Hydrocen Project 5.2.7 Measurement, calculation and modelling of dynamics and dynamic loading in hydropower systems

Appendix A. The relative velocity *W*

We will find an expression for the relative velocity W using the Euler equation (Not to be mistaken with the Euler *pump and turbine* equation), including the potential function $\varphi = \omega r V_\theta$. We will be focusing on the radial direction component of the N.-S. equations and the gradient of the potential function in radial direction is thus

$$\frac{\partial \varphi}{\partial r} = \frac{\partial (uV_\theta)}{\partial r} = \omega \frac{\partial (rV_\theta)}{\partial r} = \omega V_\theta + \omega r \frac{\partial V_\theta}{\partial r} = \omega(W_\theta + \omega r) + \omega r \frac{\partial}{\partial r}(W_\theta + \omega r) = \omega W_\theta + \omega r \frac{\partial W_\theta}{\partial r} + 2\omega^2 r \quad (A1)$$

Where it has been used that the component of absolute velocity in the circumferential direction is linked to the rotation of the runner and the relative velocity by $V_\theta = W_\theta + \omega r$. Substituting this into Eq. 1 we get

$$\frac{1}{\rho}\frac{\partial p}{\partial r} = -\frac{\partial V_r}{\partial t} - V_r \frac{\partial V_r}{\partial r} - \frac{(W_\theta + \omega r)}{r}\frac{\partial V_r}{\partial \theta} + \frac{(W_\theta + \omega r)^2}{r} - V_z \frac{\partial V_r}{\partial z} - \omega W_\theta - \omega r \frac{\partial W_\theta}{\partial r} - 2\omega^2 r \quad (A2)$$

At the outlet section under investigation, we assume no radial component of the flow, meaning we assume it is turned into an axial flow exactly at this cross section (V_z=V_m). We further assume axisymmetric conditions, as well as steady state conditions. This reduces the above equation to

$$\frac{1}{\rho}\frac{\partial p}{\partial r} = -a_{abs,r} - \frac{\partial \varphi}{\partial r} = \frac{W_\theta^2}{r} - V_m \frac{\partial V_r}{\partial z} + \omega W_\theta - \omega^2 r - \omega r \frac{\partial W_\theta}{\partial r} \quad (A3)$$

The second term on the right-hand side, $V_m \frac{\partial V_r}{\partial z}$, requires some attention. It stems from the absolute acceleration, and the link between absolute acceleration and relative acceleration is given as

$$\vec{a}_{abs} = \vec{a}_{rel} + \vec{a}_{corriolis} + \vec{a}_{centripetal} = \vec{a}_{rel} + 2\vec{\omega} \times \vec{W} + \vec{\omega} \times (\vec{\omega} \times \vec{r}) \quad (A4)$$

And in the radial direction

$$a_{abs,r} = a_{rel,r} + a_{corriolis,r} + a_{centripetal,r} = a_{rel,r} - 2\omega W_\theta - \omega^2 r \quad (A5)$$

Finding the relative acceleration's component in the radial direction we can turn to a relative frame of reference, as viewed in Figure 1. We realize that the flow crossing the cross section under investigation experience two accelerations, one in towards the axis of rotation due to the component of relative velocity in the circumferential direction, $-\frac{W_\theta^2}{r}$, and another one out from the axis of the rotation due to the curvature of the streamline at this section, $\frac{W_m^2}{\hat{r}}$, where $\hat{r}$ is the radius of curvature of the streamline at this section;

$$a_{rel,r} = \frac{\hat{W}_m^2}{r} - \frac{W_\theta^2}{r} \quad (A6)$$

If our frame of reference is relative to the rotation of the runner and considering the outlet as the end of a curved channel similar to sketched in Figure 1, we can describe the acceleration in the radial direction in this relative frame of reference as $a_{rel,r}$, as

$$-\frac{W_\theta^2}{r} - 2\omega W_\theta - \omega^2 r + V_m \frac{\partial V_r}{\partial z} = \frac{\hat{W}_m^2}{r} - \frac{W_\theta^2}{r} - 2\omega W_\theta - \omega^2 r \tag{A7}$$

We see that

$$V_m \frac{\partial V_r}{\partial z} = \frac{\hat{W}_m^2}{r} \tag{A8}$$

We substitute back into Eq. A3 and get

$$\frac{1}{\rho}\frac{\partial p}{\partial r} = \frac{W_\theta^2}{r} - \frac{\hat{W}_m^2}{r} + \omega W_\theta - \omega^2 r - \omega r \frac{\partial W_\theta}{\partial r} \tag{A9}$$

This can be integrated to obtain an expression for the pressure difference from points 2b to 2a. Assuming that the streamlines follow the path of concentrical circles when crossing the outlet cross section, the radius of curvature $\hat{r}$ is the fixed radius value r_c plus the negative of the increment in radial position. Using this to integrate Eq. A9 from the smallest outlet radius (at 2b) to the largest outlet radius (at 2a) one finds an expression for the pressure difference

$$\frac{p_{2a} - p_{2b}}{\rho} = -\int_{2b}^{2a} \frac{W_m^2}{r_c - r} dr + \int_{2b}^{2a} \frac{W_\theta^2}{r} dr + \int_{2b}^{2a} \omega W_\theta dr - \int_{2b}^{2a} \omega r \frac{\partial W_\theta}{\partial r} dr - \int_{2b}^{2a} \omega^2 r dr \tag{A10}$$

We can also get an expression for the pressure difference by applying the *rothalpy equation, aka Bernoulli in a rotating frame,* between points 1a to 2a, and from 1b to 2b, solving for pressures in 2a and 2b and taking the difference. The rothalpy equation is a version of the Bernoulli equation for flow observed from a rotating inertial frame. It compensates for the fact that we are able to observe the pressure due to the rotational motion even if the rotational speed is invisible to us and the fact that this pressure is not able to accelerate the relative flow; the velocity we can observe is no longer the velocity from the stationary frame, we can only observe the relative velocity; The last important feature of the equation is that it describes the relative energy content of the flow, and use the fact that this is constant, *even if energy is extracted from the absolute reference frame flow.* Points 1a and 1b are at points where the flow is parallel and is not yet being diverted downwards, hence the only pressure difference between them is the static contribution of the water column from point 1b to 1a. This contribution in very small compared to the other terms, and neglecting this yields $p_{1a}=p_{1b}$, and in fact the elevation term in the Bernoulli equation can be omitted altogether, as the potential in the Euler equation also has omitted gravity. The velocities at 1a and 1b can also be regarded as the same. Using the rothalpy equation twice, solving for the pressures at point 2a and 2b, and taking the difference between them one finds

$$p_{1a} - \rho\frac{\omega^2 r_{1a}^2}{2} + \rho\frac{W_{1a}^2}{2} = p_{2a} - \rho\frac{\omega^2 r_{2a}^2}{2} + \rho\frac{W_{2a}^2}{2} \tag{A11}$$

$$p_{2a} = p_{1a} + \frac{\rho}{2}(W_{1a}^2 - \omega^2 r_{1a}^2 + \omega^2 r_{2a}^2 - W_{2a}^2) \tag{A12}$$

$$p_{1b} - \rho\frac{\omega^2 r_{1b}^2}{2} + \rho\frac{W_{1b}^2}{2} = p_{2b} - \rho\frac{\omega^2 r_{2b}^2}{2} + \rho\frac{W_{2b}^2}{2} \tag{A13}$$

$$p_{2b} = p_{1b} + \frac{\rho}{2}\left(W_{1b}^2 - \omega^2 r_{1b}^2 + \omega^2 r_{2b}^2 - W_{2b}^2\right) \tag{A14}$$

$$p_{2a} - p_{2b} = p_{1a} + \frac{\rho}{2}(W_{1a}^2 - \omega^2 r_{1a}^2 + \omega^2 r_{2a}^2 - W_{2a}^2) - \left(p_{1b} + \frac{\rho}{2}\left(W_{1b}^2 - \omega^2 r_{1b}^2 + \omega^2 r_{2b}^2 - W_{2b}^2\right)\right) \quad (A15)$$

$$p_{2a} - p_{2b} = p_{1a} - p_{1b} + \frac{\rho}{2}(W_{1a}^2 - W_{1b}^2 + \omega^2 r_{1b}^2 - \omega^2 r_{1a}^2 + \omega^2 r_{2a}^2 - \omega^2 r_{2b}^2 + W_{2b}^2 - W_{2a}^2) \quad (A16)$$

$$p_{2a} - p_{2b} = \frac{\rho}{2}\left(\omega^2 r_{2a}^2 - \omega^2 r_{2b}^2 - \left(W_{2a}^2 - W_{2b}^2\right)\right) \quad (A17)$$

This appears to be the integration of differential pressure from b to a and the pressure differential can be written as

$$\frac{p_{2a} - p_{2b}}{\rho} = \int_{2b}^{2a} \omega^2 r dr - \int_{2b}^{2a} W dW \quad (A18)$$

Setting the expression for the pressure differential equal will yield the following integral relation

$$-\int_{2b}^{2a} \frac{W_m^2}{r_c - r} dr + \int_{2b}^{2a} \frac{W_\theta^2}{r} dr + \int_{2b}^{2a} \omega W_\theta dr - \int_{2b}^{2a} \omega r \frac{\partial W_\theta}{\partial r} dr - \int_{2b}^{2a} \omega^2 r dr = \int_{2b}^{2a} \omega^2 r dr - \int_{2b}^{2a} W dW \quad (A19)$$

All integral limits are the same and we can look at the differential relation instead

$$-\frac{W_m^2}{r_c - r} dr + \frac{W_\theta^2}{r} dr + \omega W_\theta dr - 2\omega^2 r dr - \omega r dW_\theta = -W dW \quad (A20)$$

The components W_m and W_θ of the relative velocity are linked to the relative velocity by the blade outlet angle beta through the geometrical relations in the velocity triangle, $W_m = W \sin\beta$ and $W_\theta = W \cos\beta$

$$\frac{W_m^2}{r_c - r} dr - \frac{W_\theta^2}{r} dr - \omega W_\theta dr + 2\omega^2 r dr = (W - \omega r cos\beta) dW \quad (A21)$$

Rearranging, we can write

$$\frac{W^2\left(\frac{sin^2\beta}{r_c - r} - \frac{cos^2\beta}{r}\right) - \omega W cos\beta + 2\omega^2 r}{(W - \omega r cos\beta)} dr = dW \quad (A22)$$

$$\frac{dW}{dr} = \frac{W^2\left(\frac{sin^2\beta}{r_c - r} - \frac{cos^2\beta}{r}\right) - \omega W cos\beta + 2\omega^2 r}{(W - \omega r cos\beta)} \quad (A23)$$

Appendix B. Numerical investigations

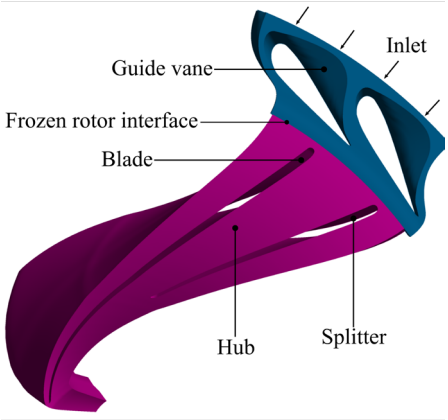

Figure B1 :Computational domain of the turbine. Draft tube is not shown.

For numerical investigations, a high head model Francis turbine, Francis-99, is considered. The computational domain consists of guide vanes, runner and draft tube. Hexahedral mesh was created in the turbine. Figure A1 shows computational domain of guide vane and runner. The mesh in the guide vane and the blade passages was created using ANSYS® TurboGrid™, whereas mesh in the draft tube was created using ANSYS® ICEM CFD™. A passage modelling approach is considered, which includes two guide vanes, a blade, a splitter and a draft tube. A periodic boundary condition was considered for the guide vanes and the runner. This allows information transfer on both sides of the periodicity. Furthermore, to connect stationary (guide vane and draft tube) domains to the rotating domain (runner), a rotating reference frame method, frozen rotor type, is considered. Though, this method is not true transient type, it allows data exchange at fixed position of the runner, and it does not average over the complete circumference of the runner. Data exchange takes place at the corresponding fixed locations of the interface and wake effect from the guide vanes can be modelled, if any. The simulations are conducted using ANSYS® CFX®, where all parameters related to the turbulence model were deactivated. The viscosity of water was set close to zero. Steady state simulations of the turbine are conducted. The present focus is only the best efficiency point (BEP). The parameters of BEP are shown in Table A1.

Table B1. Range of parameters and boundary condition for simulation

#	Load	Guide vane	Net head	Runner speed	Inlet pressure	Outlet pressure
1	BEP	10°	30 m	531.6 rpm	3.4714 bar	0.5684

Available experimental data of model test (see Figure A2) are used to prescribe the boundary conditions in simulations. The numerical model is verified and validated with the experimental data at BEP and part load operations. Computed discretization error is 0.5%. The error is determined using grid convergence index method [5] with respect to hydraulic efficiency and torque values. Complete description on the mesh independency study and the validation is presented in a previous publication [6]. The validation is performed with complete turbine, which includes complete spiral casing, stay vanes, 28 guide vanes. 15 blades, 15 splitters and draft tube. The selected mesh contains around 2 million nodes in the turbine of one blade channel and the one guide vane channel. Guide vane passage, blade passage and draft tube contains, 0.35, 0.19 and 1.4 million nodes, respectively.

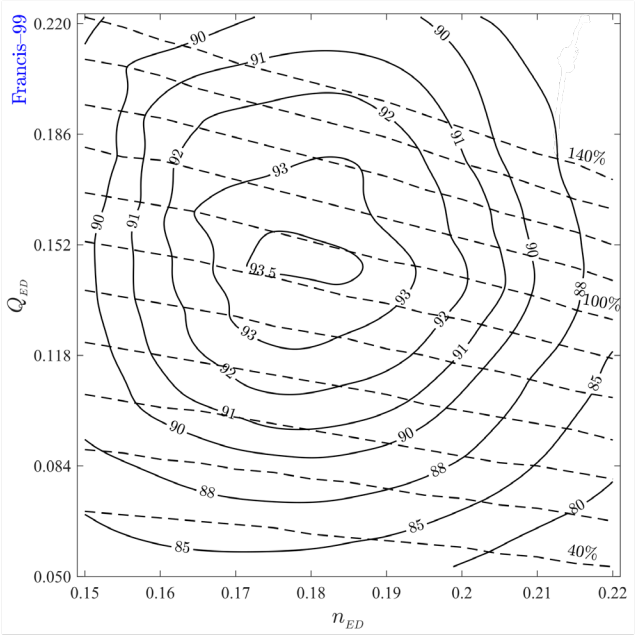

Figure B2. Iso-efficiency diagram of the model Francis turbine. The diagram is reproduced using available experimental data of the model performance test according to IEC 60193 in the Waterpower laboratory. Efficiency is presented in percentage; dash line indicates guide vane opening in percentage.

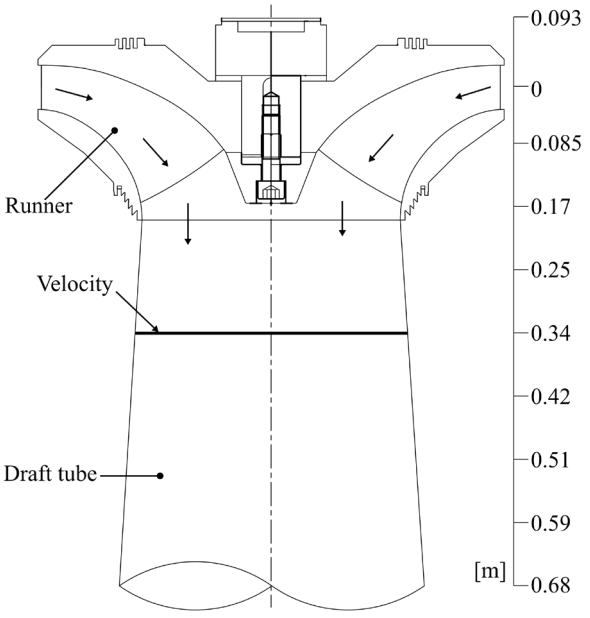

Figure B3. Illustration of a model Francis turbine indicating the location of velocity data line in the draft tube.

Appendix C. Draft tube losses

The energy equation (units power) is obtained applying the Reynolds transport theorem using the hydraulic mechanical energy E_{mech} as the extensive property which go into the equation [9]. This is seen in the equation below, where $e = E_{mech}/m$, being the specific hydraulic mechanical energy, $e = \frac{p}{\rho} + \frac{V^2}{2}$.

$$\frac{dE_{mech}}{dt} = \frac{d}{dt}\int_{CV} \rho e d\forall + \int_{CS} \rho e\left(\overrightarrow{V_r}\cdot\vec{n}\right)dA \qquad (C\ 1)$$

Applying this between the cross section where we know the velocity distribution and the lower reservoir where the water has settled assuming steady state we can write

$$\rho g Q\left(h_{loss,draft\ tube} + h_{loss,tailrace} + h_{outlet}\right) = \int_{\substack{inlet\\draft\ tube}} \left(p + \rho\frac{V_m^2 + V_\theta^2}{2}\right)V_m dA - \rho g Q h_{tailwater} \qquad (C\ 2)$$

Unfortunately, we don't know the pressure in the inlet of the draft tube, we only have information on the pressure gradient. We're missing a boundary condition to be able to find the exact pressure distribution. If we have a uniform flow without any swirl the pressure would be uniform and the pressure gradient in the radial direction would be zero. Integrating this zero-gradient would only return a constant, and this constant would have been determined to be the pressure of the swirl-free flow. This pressure is easily linked to the losses in axisymmetric flows, as determined by friction factor or Manning number application. Investigating this flow case using the energy equation from the inlet of the draft tube to the outlet of the tailrace tunnel at the power plant we can write

$$\begin{aligned}\rho g Q\left(h_{loss,draft\ tube,z} + h_{loss,tailrace,z} + h_{outlet,z}\right) &= \int_{\substack{inlet\\draft\ tube}} \left(p_{uni} + \rho\frac{Q^2}{2A^2}\right)\frac{Q}{A}dA - \rho g Q h_{tailwater} \\ &= p_{uni}Q + \rho\frac{Q^3}{2A_{\substack{inlet\\dt}}^2} - \rho g Q h_{tailwater}\end{aligned} \qquad (C\ 3)$$

The axial losses on the left-hand side are easy to calculate using standard equations for pipe flow. In practice the only unknown in this equation is the uniform pressure term p_{uni}.

$$p_{uni}Q = \rho g Q\left(h_{loss,draft\ tube,z} + h_{loss,tailrace,z} + h_{outlet,z}\right) - \rho\frac{Q^3}{2A_{\substack{inlet\\dt}}^2} + \rho g Q h_{tailwater} \qquad (C\ 4)$$

So, we could solve for this, and use as a condition for the pressure at the radius r_m where the local meridional velocity V_m=Q/A, as for the uniform flow assumption, when integrating the pressure gradient. The pressure would then be

$$p = \int \frac{\partial p}{\partial r}dr + p_{uni} - \int_{r=0}^{r_m} \frac{\partial p}{\partial r}dr \qquad (C\ 5)$$

Where the latter integral is definite returning the value of the pressure differential from the centre to r_m, to correct for the pressure p_{uni} not being the constant value to add to the distribution at r=0, but at r= r_m. We can substitute back into Eq. C2 and get

$$\begin{aligned}
&\rho g Q\left(h_{loss,draft\ tube} + h_{loss,tailrace} + h_{outlet}\right) \\
&\quad = \int_{\substack{inlet \\ draft\ tube}} \left(\int \frac{\partial p}{\partial r} dr + p_{uni} - \int_{r=0}^{r_m} \frac{\partial p}{\partial r} dr + \rho \frac{V_m^2 + V_\theta^2}{2} \right) V_m dA \\
&\quad - \rho g Q h_{tailwater} \\
&\quad = p_{uni} Q + \int_{\substack{inlet \\ draft\ tube}} \left(\int \frac{\partial p}{\partial r} dr - \int_{r=0}^{r_m} \frac{\partial p}{\partial r} dr + \rho \frac{V_m^2 + V_\theta^2}{2} \right) V_m dA \\
&\quad - \rho g Q h_{tailwater} \\
&\quad = \rho g Q\left(h_{loss,draft\ tube,z} + h_{loss,tailrace,z} + h_{outlet,z}\right) \\
&\quad + \int_{\substack{inlet \\ draft\ tube}} \left(\int \frac{\partial p}{\partial r} dr - \int_{r=0}^{r_m} \frac{\partial p}{\partial r} dr + \rho \frac{V_m^2 + V_\theta^2}{2} \right) V_m dA \\
&\quad - \rho \frac{Q^3}{2A_{\substack{inlet \\ dt}}^2}
\end{aligned} \tag{C 6}$$

Solving for the head loss in the draft tube, we can write

$$\begin{aligned}
&\rho g Q h_{loss,draft\ tube} \\
&\quad = \rho g Q\left(h_{loss,draft\ tube,z} + h_{loss,tailrace,z} - h_{loss,tailrace}\right. \\
&\quad \left. + h_{outlet,z} - h_{outlet}\right) \\
&\quad + \int_{\substack{inlet \\ draft\ tube}} \left(\int \frac{\partial p}{\partial r} dr - \int_{r=0}^{r_m} \frac{\partial p}{\partial r} dr + \rho \frac{V_m^2 + V_\theta^2}{2} \right) V_m dA \\
&\quad - \rho \frac{Q^3}{2A_{\substack{inlet \\ dt}}^2}
\end{aligned} \tag{C 7}$$

Where the difference between the total losses and the axial losses must be the losses due to loss of rotation, which we use subscript θ to indicate. These losses might be difficult to quantify and assign to either tailrace or outlet, but at the outlet all the kinetic energy is lost, also the rotational component. It's really not important to know where these losses occur either, because the origin of the rotation is the turbine runner, and the losses due to loss of rotation should be assigned to the turbine unit altogether. Therefore, all the flux of the rotational velocity component at the inlet of the draft tube is said to be these losses,

$$\begin{aligned}
&h_{loss,tailrace} - h_{loss,tailrace,z} + h_{outlet} + h_{outlet,z} = h_{loss,tailrace,\theta} + h_{outlet,\theta} \\
&\quad = \int_{\substack{inlet \\ draft\ tube}} \rho \frac{V_\theta^2}{2} V_m dA
\end{aligned} \tag{C 8}$$

$$
\begin{aligned}
&\rho g Q h_{loss,draft\ tube} \\
&= \rho g Q h_{loss,draft\ tube,z} - \int\limits_{\substack{inlet \\ draft\ tube}} \rho \frac{V_\theta^2}{2} V_m dA \\
&+ \int\limits_{\substack{inlet \\ draft\ tube}} \left(\int \frac{\partial p}{\partial r} dr - \int\limits_{r=0}^{r_m} \frac{\partial p}{\partial r} dr + \rho \frac{V_m^2 + V_\theta^2}{2} \right) V_m dA \\
&- \rho \frac{Q^3}{2A_{\substack{inlet \\ dt}}^2} \\
&= \rho g Q h_{loss,draft\ tube,z} \\
&+ \int\limits_{\substack{inlet \\ draft\ tube}} \left(\int \frac{\partial p}{\partial r} dr - \int\limits_{r=0}^{r_m} \frac{\partial p}{\partial r} dr + \rho \frac{V_m^2}{2} \right) V_m dA - \rho \frac{Q^3}{2A_{\substack{inlet \\ dt}}^2}
\end{aligned}
\qquad (C\ 9)
$$

If the flow is uniform, the pressure gradient is zero and the two pressure gradient integrals are zero, the latter term inside the integral becomes identical to the last term on the right-hand side and they cancel out, leaving only

$$\rho g Q h_{loss,draft\ tube} = \rho g Q h_{loss,draft\ tube,z} \qquad (C\ 10)$$

Which is as should be if there is no rotation in the flow; the losses would be purely linked to axial flow.

8. References

[1] Giosio, D.R., et al., *Physics-Based Hydraulic Turbine Model for System Dynamic Studies.* IEEE Transactions on Power Systems, 2017. **32**(2): p. 1161-1168.
[2] Storli, P.-T. and T.K. Nielsen, *Simulation and Discussion of Models for Hydraulic Francis Turbine Simulations.* IFAC-PapersOnLine, 2018. **51**(2): p. 109-114.
[3] Nielsen, T.K., *Simulation model for Francis and Reversible Pump Turbines.* International Journal of Fluid Machinery and Systems, 2015. **8**(3): p. 169-182.
[4] Nielsen, T.K. and P. Storli. *Measurements and simulations of turbines on common grid*. in *IOP Conference Series: Earth and Environmental Science*. 2014. IOP Publishing.
[5] Nielsen, T.K. *Dynamic Behaviour of Governing Turbines Sharing the Same Electrical Grid*. in *18th IAHR Symposium on Hydraulic Machinery and Cavitation*. 1996. Valencia: Kluwer Acafdemic Publisher.
[6] Nielsen, T.K., *Transient characteristics of High Head Francis Turbines*. 1990, NTH.
[7] Yuan, S.W., *Foundations of fluid mechanics*. Civil engineering and engineering mechanics series. 1967, Englewood Cliffs, N.J: Prentice-Hall.
[8] Brekke, H., J.T. Billdal, and Anderson, in *Strømningsmaskinteori*, H. Brekke, Editor., NTNU
[9] Cengel, Y.A. and J.M. Cimbala, *Fluid Mechanics, Fundamentals and Applications*. 2014: McGraw Hill education.
[10] Agnalt, E., et al., *The Rotor-Stator Interaction Onboard a Low Specific speed Francis Turbine.* International Journal of Fluid Machinery and Systems, 2020. **13**(2): p. 302-309.
[11] Stepanoff, A.J., *Centrifugal and axial flow pumps : theory, design, and application*. 2nd ed. ed. 1957, New York: Wiley.
[12] Dahlhaug, O.G., *A study of swirl flow in draft tubes*. 1997, Division of Thermal Energy and Hydropower, Norwegian University of Science and Technology: Trondheim.